35th Annual International Conference of the IEEE EMBS
Osaka, Japan, 3 - 7 July, 2013

Internal Inconsistencies in Models of Electrical Stimulation in Neural Tissue

Hamish Meffin[1,2,3], Bahman Tahayori[1,2,*], *Member, IEEE*,
David B. Grayden[1,2,3,4], *Member, IEEE*, Anthony N. Burkitt[1,2,3,4], *Senior Member, IEEE*

***Abstract*— Calculating the membrane potential of a neurite under extracellular electrical stimulation is important in the design of some recent stimulation strategies for neuroprosthetic devices including retinal implants, cochlear implants, deep brain stimulation. A common approach, widely used in the electrical stimulation literature uses a volume conductor model to calculate the electrical potential in the tissue and then extracts the voltage or current density on the surface of a neuron, which is used as input to the cable equation to calculate the neuron's response. However this approach ignores the effect of the neuron itself as well as surrounding neurons on the extracellular potential. Here we highlight that this leads to an internal inconsistency in the overall model because the result depends on whether the voltage or current density is used to calculate the neural response. The magnitude of this discrepancy is calculated for the example of a point source electrode in a homogeneous medium and is shown to be up to several hundred percent under some stimulus conditions. The inconsistency can be resolved by ensuring that the voltage is related to the current density by the transimpedance of the neurite. Deriving a volume conductor model that satisfies this relationship requires further work.**

I. INTRODUCTION

Extracellular electrical stimulation of neurons is widely used in neuroprosthetic devices such as cochlear implants, retinal implants, cortical and deep brain stimulators [1], [2], [3]. Modeling extracellular electrical stimulation of neurons is an important step in the design of stimulation techniques for such devices, and, therefore, has gained considerable attention in the literature [4], [5], [6], [7].

A common approach for calculating the membrane potential is based on a two-stage model, a volume conductor, stimulating electrodes and one or more neuron under stimulation. In the first stage of the model, the extracellular potential and current density in the tissue due to electrical stimulation are calculated. Typically the effect of the neurite is ignored and the extracellular potential is calculated in the absence of the neurite. While it is possible to include one or a few neurites in the volume conductor, the situation becomes computationally intractable once many neurons are included so as to model the spatial spread of excitation. In the second stage, either the extracellular voltage or the extracellular current density on the surface of the neurite is extracted from the first stage, and used as the boundary condition to calculate the membrane potential using available models such as the cable equation [4], [8], [6].

In principle, for the modelling approach to be internally consistent, it should not matter whether this boundary condition is described in terms of the voltage or the current density; the resulting membrane potential should be the same. However, this is generally not the case; a consequence of neglecting the effect of the neurite on the extracellular voltage and current density in stage 1 . A consistent membrane potential results if and only if the extracellular voltage is related to the extracellular current density (normal to the membrane surface) by the transimpedance of the neurite (see Eqs. (33) and (34) in [9]). These relations do not hold for general volume conductors in the absence of embedded neurites.

The objective of this paper is to quantitatively assess the degree of discrepancy in the calculated membrane potential between the two cases of voltage versus current density boundary conditions on the surface of the neurite. We do this by considering the simple example of a cylindrical neurite in a homogeneous volume conductor with stimulation by a point source electrode. The two stage model described above is followed: Stage 1 uses the standard expression for the electrical potential in a homogeneous volume conductor; Stage 2 uses the equations derived in [9], [10] for subthreshold membrane potential under the two types of boundary conditions.

II. METHODS

A. Stage 1: Point Source Stimulation in a Homogeneous Volume Conductor

Consider the cylindrical neurite of radius b, located in a homogeneous and isotropic volume with resistivity ρ_t and separated from a point source electrode by distance h as shown in Figure 1. The names of parameters and variables of the model are summarised in Table I. Ignoring the presence of the neurite on the potential, the voltage at a distance R on the neurite surface may be written as

$$V_A = \frac{\rho_t}{4\pi R} I_{\mathrm{A}}(t), \tag{1}$$

or equivalently in terms of the current density,

$$\mathbf{J}_{\mathrm{A}} = \frac{I_{\mathrm{A}}(t)}{4\pi R^3}\mathbf{R}, \tag{2}$$

where $\mathbf{R} = (b - h\cos\theta)\,\mathbf{e}_r + h\sin\theta\,\mathbf{e}_\theta + z\,\mathbf{e}_z$ in cylindrical polar coordinates (r, z, θ). In the above equations, $I_A(t)$ is

[1]NeuroEngineering Laboratory, Department of Electrical and Electronic Engineering, The University of Melbourne, Parkville, VIC 3010, Australia. [2]Centre for Neural Engineering, The University of Melbourne, Parkville, VIC 3010, Australia. [3]NICTA Victoria Research Labs, The University of Melbourne, Parkville, VIC, 3010, Australia. [4]Bionics Institute 384-388 Albert Street, East Melbourne, VIC 3002. *Corresponding author, bahmant@unimelb.edu.au.

978-1-4577-0216-7/13/$26.00 ©2013 IEEE

TABLE I

PARAMETERS OF THE MODEL SHOWN IN FIGURE 1.

Parameter	Description	Unit
a	Neurite radius	m
b	Outer cylinder radius	m
d	Width of the extracellular sheath, $d = b - a$	m
ρ_i	Intracellular space resistivity	Ω·m
ρ_e	Extracellular space resistivity	Ω·m
r_i	Intracellular resistance, $r_i = \rho_i/\pi a^2$	Ω/m
r_e	Extracellular resistance, $r_e = \rho_e/\pi(b^2 - a^2)$	Ω/m
R_M	Membrane's unit area resistance	Ω·m^2
r_M	Membrane's resistance, $r_M = R_M/2\pi a$	Ω·m
C_M	Membrane's capacitance per unit area	F/m^2
h	Electrode distance from the neurite axis	m
I_A	Electrode current	A
J_A	Current density on outer cylinder boundary	A/m^2
V_A	Voltage across the outer cylinder	V
V_M	The membrane potential	V

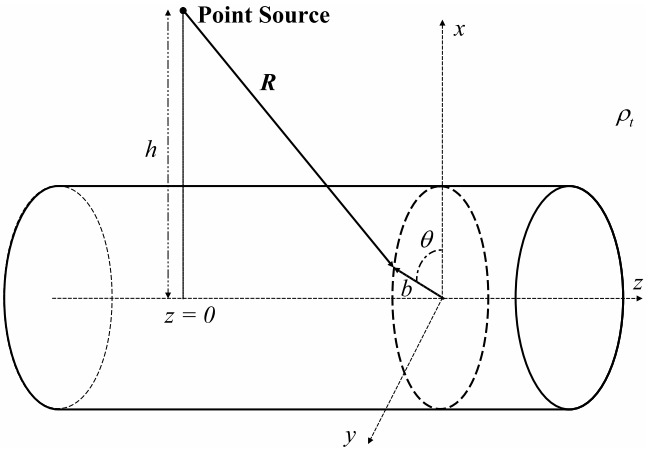

Fig. 1. Model of point source stimulation of a cylindrical neurite. Parameters of the model are described in Table I.

the applied current waveform, and $\mathbf{e}_r$, $\mathbf{e}_\theta$ and $\mathbf{e}_z$ are unit vectors in the r, θ and z directions, respectively.

B. Stage 2: Calculation of Subthreshold Membrane Potential

The equations describing the subthreshold membrane potential under voltage and current density boundary conditions are given below and were derived in [9], [10]. They involve two modes of stimulation: a longitudinal mode, which is the conventional mode described by a classical cable equation, and a transverse mode, which is often neglected and is described by an ordinary differential equation in time. These modes of stimulation are illustrated schematically in Figure 2 (see [9] for a full discussion). It should be emphasised that our basic conclusions are unaltered if we consider only the conventional longitudinal mode. The modes can be combined in a Fourier series to give the total membrane potential:

$$V_{\mathrm{M}}(z,\theta,t) = \sum_{n=-\infty}^{\infty} \bar{V}_{\mathrm{M}}(z,n,t)e^{jn\theta} \tag{3}$$

where

$$\bar{V}_{\mathrm{M}}(z,n,t) = \frac{1}{2\pi}\int_{2\pi} V_{\mathrm{M}}\, e^{-jn\theta}\, d\theta. \tag{4}$$

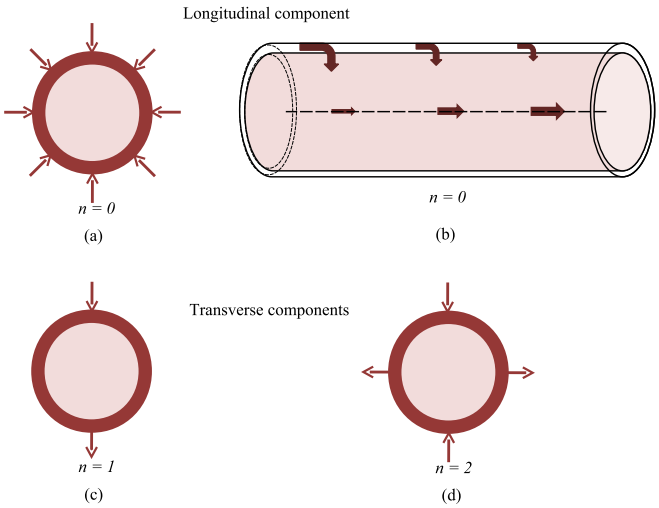

Fig. 2. Illustration of the different modes of stimulations including the $n = 0$ longitudinal mode, (a) and (b), and transverse modes for (c) $n = 1$ and (d) $n = 2$. Arrows indicate the direction of current flow, dark red indicates the extracellular space and light red the intracellular space. The longitudinal mode involves current entering the neurite axisymmetrically and passing along it. The transverse modes involve current passing across the neurite. Higher order modes, e.g. $n = 2$, are possible but typically make minor contributions.

Typically only the $n = 0$ longitudinal mode, and the $n = \pm 1$ major transverse mode make significant contribution to the membrane potential. For these two modes we use the notation $\overline{V}_{\mathrm{M}}(z, n = 0, t) = V_{\mathrm{M}}^{\parallel}$ and $\overline{V}_{\mathrm{M}}(z, n = 1, t) = V_{\mathrm{M}}^{\perp}$.

We consider stimulation with symmetric biphasic current pulses, with pulse phase duration from 10 μs to 100 ms and no interphase gap. For pulses of these durations the transverse mode of stimulation follows the time course of the pulse almost instantaneously, so that we use a quasi-stationary approximation to the ordinary differential equation describing this mode in the following.

1) Current Density Boundary Conditions:

Longitudinal Mode:

$$\lambda_{0_J}^2 \frac{\partial^2 \bar{V}_{\mathrm{M}}^{\parallel}}{\partial z^2} - \tau_{\mathrm{M}} \frac{\partial \bar{V}_{\mathrm{M}}^{\parallel}}{\partial t} - \bar{V}_{\mathrm{M}}^{\parallel} = -2\pi r_e b \lambda_{0_J}^2 \bar{J}_{\mathrm{A}}^{\parallel}, \tag{5}$$

in which the electrotonic length constant and the membrane time constant are

$$\lambda_{0_J}^2 \triangleq \frac{r_{\mathrm{M}}}{r_{\mathrm{e}} + r_{\mathrm{i}}} \qquad \text{and} \qquad \tau_{\mathrm{M}} \triangleq R_{\mathrm{M}} C_{\mathrm{M}}. \tag{6}$$

Transverse mode:

$$\bar{V}_{\mathrm{M}}^{\perp} = \frac{\rho_{\mathrm{e}} b^2}{d} \bar{J}_{\mathrm{A}}^{\perp}. \tag{7}$$

The current density boundary conditions enter through the right hand sides of equations (5) and (7) via $\bar{J}_{\mathrm{A}}^{\parallel}$ and $\bar{J}_{\mathrm{A}}^{\perp}$. Using equation (2) and a Taylor's expansion in the b/h, together with equation (4), we find the longitudinal and transverse components of the current density on the cylinder

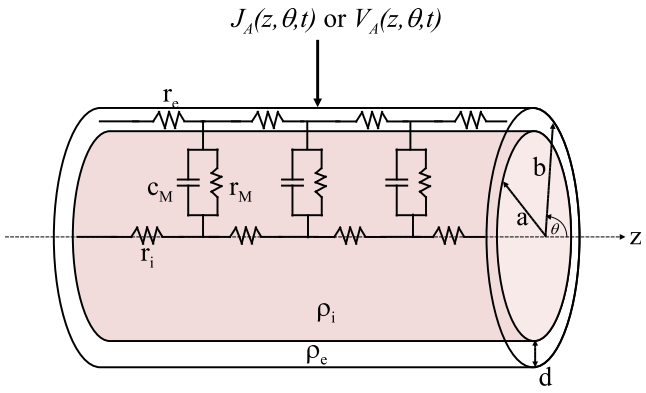

Fig. 3. Cylindrical model of a neurite. The inner cylinder represents the intracellular region and the extracellular space is modeled by a thin sheath with width d. The parameters of the model are described in Table I and their values given in Table II.

surface:

$$\bar{J}_{\mathrm{A}}^{\parallel} = \frac{I_{\mathrm{A}}(t)}{8\pi} \frac{b(2z^2 - h^2)}{(h^2 + z^2)^{\frac{5}{2}}}, \tag{8a}$$

$$\bar{J}_{\mathrm{A}}^{\perp} = -\frac{I_{\mathrm{A}}(t)}{8\pi} \frac{h}{(h^2 + z^2)^{\frac{3}{2}}}. \tag{8b}$$

2) Voltage Boundary Conditions:

Longitudinal Mode:

$$\lambda_{0_V}^2 \frac{\partial^2 \bar{V}_{\mathrm{M}}^{\parallel}}{\partial z^2} - \tau_{\mathrm{M}} \frac{\partial \bar{V}_{\mathrm{M}}^{\parallel}}{\partial t} - \bar{V}_{\mathrm{M}}^{\parallel} = -\lambda_{0_V}^2 \frac{\partial^2 \bar{V}_{\mathrm{A}}^{\parallel}}{\partial z^2}, \tag{9}$$

where

$$\lambda_{0_V}^2 = \frac{R_M}{2\pi a r_i} = \frac{r_M}{r_i}. \tag{10}$$

Note that electrotonic length constant for voltage boundary conditions, λ_{0_V}, is larger than it counterpart for current density boundary conditions, λ_{0_J}.

Transverse Mode:

$$\bar{V}_{\mathrm{M}}^{\perp} = -\bar{V}_{\mathrm{A}}^{\perp} \tag{11}$$

Assuming $\frac{b}{h} \ll 1$ and using Taylor series expansion, the longitudinal and transverse components of the voltage boundary conditions are calculated to be

$$\bar{V}_{\mathrm{A}}^{\parallel} = \frac{I_{\mathrm{A}}(t)\rho_t}{4\pi(h^2 + z^2)^{1/2}} \tag{12a}$$

$$\bar{V}_{\mathrm{M}}^{\perp} = \frac{I_{\mathrm{A}}(t)\rho_t\, b\, h}{8\pi(h^2 + z^2)^{3/2}}. \tag{12b}$$

Equations (5)-(12) were solved for $\bar{V}_{\mathrm{M}}$ in the z and t Fourier domains and the resulting expressions numerically inverse Fourier transformed in Matlab. Results were also checked against simulations in COMSOL with discrepancy less than a few percent (results not shown).

III. Results

An example showing a comparison between the calculated membrane potential for voltage versus current density boundary conditions is shown in Figure 4, for the case of a biphasic pulse with 0.1 ms phase duration, 50 mA amplitude and with the electrode 1000 μm distant from the neurite (other parameters are given in Table II). For each boundary condition the longitudinal and transverse modes are shown separately (notice that the longitudinal mode is rotationally symmetric around the cylinder, whereas the transverse mode is depolarised and hyperpolarised on opposing sides of the cylinder). The maximal depolarisation differs by nearly a factor of 10 for the longitudinal mode and by around 50% in the case of the transverse mode. Furthermore, for current density boundary conditions the transverse mode is predicted to be dominant, while for the voltage boundary conditions the longitudinal mode is predicted to be dominant. The predictions of the model are therefore both quantitatively and qualitatively inconsistent.

TABLE II

Model parameters used in simulations.

Parameter	a	b	d	C_M
Value	0.325μm	0.35μm	0.025μm	1μF/cm^2
Parameter	R_M	ρ_i	ρ_e	ρ_t
Value	4.5kΩ·cm^2	100Ω·cm	100Ω·cm	1000Ω·cm

The calculated membrane potential over a wide range of pulse phase durations (10 μs -100 ms) and electrode-neurite separations (1 μm - 1 mm) is compared in Figure 5 by plotting the ratio of the maximal membrane potential for current density versus voltage boundary conditions. For most choices of separation and pulse duration there is a large discrepancy in the maximal membrane potential between current density and voltage boundary conditions. The maximal discrepancy exceeds a 5-fold difference (ratio of 0.2) for separations of 100-1000 μm and pulse durations from 100-1000 μs, which are highly relevant to parameter ranges for many clinical applications. Generally, it is only possible to achieve agreement between results for current density and voltage boundary conditions (i.e. a ratio of 1) over a narrow range of stimulation parameters: here the parameters in Table II were chosen such that agreement occurs in the near field (when the electrode-neurite separation is under 1μm). Notice that there is a region with very short pulses and large separations for which the ratio also approaches 1 in this case.

IV. Discussion, Conclusions, and Future Work

This paper examines the commonly adopted assumption that presence of a neurite in a volume conductor can be neglected when modelling extracellular stimulation. The results show that omitting the neurite from the volume conductor leads to inconsistent results, with two calculated values of membrane potential depending on whether current density of voltage boundary conditions are used on the surface of the neural membrane. This discrepancy can be in the order of several hundred percent and is present for a large range of clinically relevant stimulation parameters.

One simple solution to this inconsistency is to restore the isolated neurite to the volume conductor and recalculate the extracellular potential [11], [12]. However, this ignores the

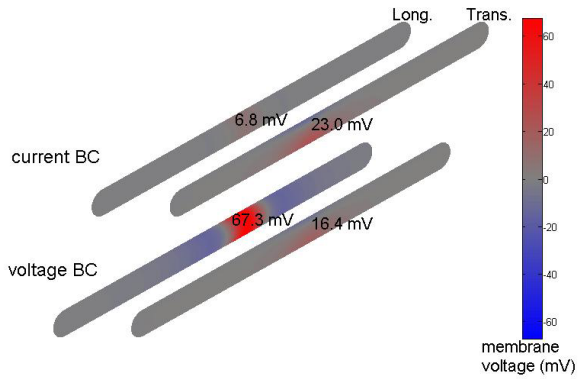

Fig. 4. Example of a comparison of the membrane potential on the neurite cylinders for current density versus voltage boundary conditions. The maximal membrane potential is marked for both longitudinal and transverse modes.

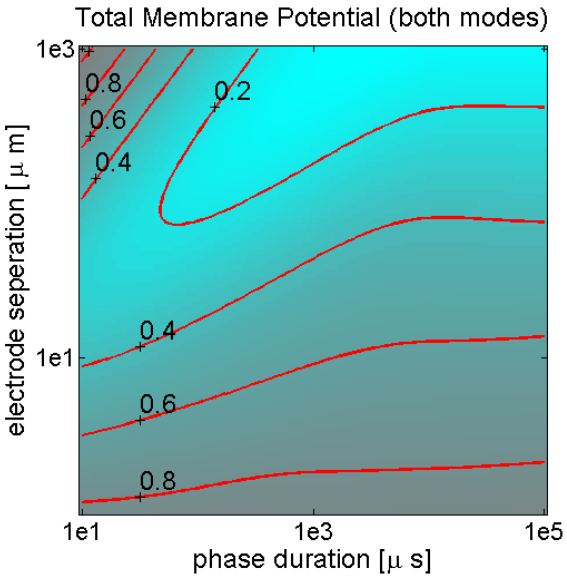

Fig. 5. Ratio of the maximal total membrane potential (longitudinal plus transverse) for current density over voltage boundary conditions as a function of phase duration in the biphasic pulse and electrode separation.

effect of neighbouring cells on both the local extracellular potential and the global flow of current. These effects have been shown to be significant using models of clustered cells in finite element model simulations [13], [14]. However, such simulations have limited applicability because the cellular packing in neural tissue is extremely close, with the extracellular gap between cells been in the order of 10s of nanometers [15]. This requires extremely small mesh sizes, which in turn results in computations with intractably large number of elements and nodes.

An alternative approach for the future may be to derive a volume conductor model that properly takes these cellular effects into account. Mathematically, consistency in the calculated membrane potential between current density and voltage boundary conditions is obtained if and only if the extracellular voltage is related to the extracellular current density by the transimpedance of the neurite plus its thin extracellular space [9]. From the transimpedance expression, it can be seen that the conductivity of the required volume conductor is not only anisotropic but also has non-trivial spatial and temporal properties. The derivation of such a volume conductor model is left to future work.

V. ACKNOWLEDGMENTS

This research was supported by the Australian Research Council (ARC) through its Special Research Initiative (SRI) in Bionic Vision Science and Technology grant to Bionic Vision Australia (BVA). The Bionics Institute acknowledges the support it receives from the Victorian Government through its Operational Infrastructure Support Program.

REFERENCES

[1] J. Niparko, *Cochlear Implants: Principles & Practices*, 2nd ed. Williams & Wilkins, 2009.

[2] J. Rizzo, J. Tombran-Tink, and C. Barnstable, *Visual Prosthesis and Ophthalmic Devices: New Hope in Sight*, ser. Ophthalmology Research. Humana, 2007.

[3] E. Montgomery, *Deep Brain Stimulation Programming: Principles and Practice*. Oxford University Press, 2010.

[4] D. McNeal, "Analysis of a model for excitation of myelinated nerve." *IEEE Transactions on Biomedical Engineering*, vol. 23, no. 4, pp. 329 – 337, 1976.

[5] F. Rattay, "Analysis of models for extracellular fiber stimulation," *IEEE Transaction on Biomedical Engineering*, vol. 36, no. 7, pp. 676–682, 1989.

[6] S. Joucla and B. Yvert, "Modeling extracellular electrical neural stimulation: From basic understanding to MEA-based applications," *Journal of Physiology-Paris*, vol. 106, pp. 146 – 158, 2012.

[7] S. Joucla, L. Rousseau, and B. Yvert, "Focalizing electrical neural stimulation with penetrating microelectrode arrays: A modeling study," *Journal of Neuroscience Methods*, vol. 209, no. 1, pp. 250 – 254, 2012.

[8] V. Schnabel and J. Struijk, "Evaluation of the cable model for electrical stimulation of unmyelinated nerve fibers." *IEEE Transactions on Bio-Medical Engineering*, vol. 48, no. 9, pp. 1027 – 1033, 2001.

[9] H. Meffin, B. Tahayori, D. Grayden, and A. Burkitt, "Modeling extracellular electrical stimulation: I. derivation and interpretation of neurite equations," *Journal of Neural Engineering*, vol. 9, p. 065005, 2012.

[10] B. Tahayori, H. Meffin, S. Dokos, D. Grayden, and A. Burkitt, "Modeling extracellular electrical stimulation: II. computational validation and numerical results," *Journal of Neural Engineering*, vol. 9, p. 065006, 2012.

[11] L. Livshitz, P. Einziger, and J. Mizrahi, "Rigorous green's function formulation for transmembrane potential induced along a 3-d infinite cylindrical cell." *IEEE Transactions on Biomedical Engineering*, vol. 49, no. 12, p. 1491, 2002.

[12] J. Gimsa and D. Wachner, "Analytical description of the transmembrane voltage induced on arbitrarily oreineted ellipsoidal and cylindrical cells," *Biophysical Journal*, vol. 81, pp. 1888–1896, 2001.

[13] M. Pavlin, N. Pavselj, and D. Miklavcic, "Dependence of induced transmembrane potential on cell density, arrangement, and cell position inside a cell system." *IEEE Transactions on Bio-Medical Engineering*, vol. 49, no. 6, pp. 605 – 612, 2002.

[14] N. Pourtaheri, W. Ying, J. Kim, and C. Henriquez, "Thresholds for transverse stimulation: fiber bundles in a uniform field." *IEEE Transactions on Neural Systems and Rehabilitation Engineering*, vol. 17, no. 5, pp. 478 – 486, 2009.

[15] E. Sykova and C. Nicholson, "Diffusion in brain extracellular space." *Physiological Reviews*, vol. 88, no. 4, pp. 1277 – 1340, 2008.